Research Article

Cancer Immunology Research

Intratumoral Delivery of TriMix mRNA Results in T-cell Activation by Cross-Presenting Dendritic Cells

Sandra Van Lint[1], Dries Renmans[1], Katrijn Broos[1], Lode Goethals[2], Sarah Maenhout[1], Daphné Benteyn[1], Cleo Goyvaerts[1], Stephanie Du Four[1], Kevin Van der Jeught[1], Lukasz Bialkowski[1], Véronique Flamand[3], Carlo Heirman[1], Kris Thielemans[1], and Karine Breckpot[1]

Abstract

Modulating the activity of tumor-infiltrating dendritic cells (TiDC) provides opportunities for novel cancer interventions. In this article, we report on our study of the uptake of mRNA by CD8α$^+$ cross-presenting TiDCs upon its intratumoral (i.t.) delivery. We exploited this property to deliver mRNA encoding the costimulatory molecule CD70, the activation stimuli CD40 ligand, and constitutively active Toll-like receptor 4, referred to as TriMix mRNA. We show that TiDCs are reprogrammed to mature antigen-presenting cells that migrate to tumor-draining lymph nodes (TDLN). TriMix stimulated antitumor T-cell responses to spontaneously engulfed cancer antigens, including a neoepitope. We show in various mouse cancer models that i.t. delivery of TriMix mRNA results in systemic therapeutic antitumor immunity. Finally, we show that the induction of antitumor responses critically depends on TiDCs, whereas it only partially depends on TDLNs. As such, we provide a platform and a mechanistic rationale for the clinical testing of i.t. administration of TriMix mRNA. *Cancer Immunol Res; 4(2); 146–56. ©2015 AACR.*

Introduction

The tumor microenvironment exerts suppressive influences on tumor-infiltrating dendritic cells (TiDC) and as such prevents induction of antitumor immunity (1, 2). It has been proposed that adjuvants like Toll-like receptor (TLR) ligands and agonistic antibodies to CD40 can restore the function of TiDCs (3–5). However, adjuvants are not TiDC-specific and could therefore evoke adverse effects when administered in an untargeted fashion. For example, intratumoral (i.t.) delivery of TLR4 ligands induces tumor cell–resistance to cytotoxic T lymphocytes (CTL), and CD40 stimulation induces neoangiogenesis of tumor blood vessels (6, 7). Consequently, strategies need to be developed that exclusively act on TiDCs, preferably on CD8α$^+$ TiDCs, which are critical for the stimulation of antitumor immunity (8, 9).

Several strategies have been developed to target adjuvants like TLR ligands or IL12, together with antigens, to cross-priming DCs (10–15). Often these exploit antibodies or nanobodies to surface markers differentially expressed by DC subsets (13, 15). Such markers include C-type lectin receptors like DEC205 and DC-SIGN (11, 12). In other cases, like in the use of DC-specific nanobodies, the target is unknown (16). These targeting moieties selectively direct the adjuvant and antigen to DCs, resulting in induction of antigen-specific immunity. However, the adjuvant and antigen coupled to isotype-matched antibodies (conjugate or nanoparticle format) or irrelevant nanobodies (lentiviral vector) evoke T-cell stimulation, *albeit* to a lesser extent (11, 12, 16). This is attributed to the ability of DCs to ingest antigens through various mechanisms. Thus, overall these strategies are not as "targeted" as anticipated. Moreover, none of these studies addressed whether adjuvants could be selectively delivered to cross-priming TiDCs without codelivery of antigens.

We developed an mRNA-based adjuvant, consisting of three mRNA molecules encoding the costimulatory molecule CD70, the activation stimulator CD40 ligand (CD40L), and constitutively active TLR4 (caTLR4), referred to as TriMix mRNA (17). Delivery of tumor-associated antigen (TAA) and TriMix mRNA to DCs, *ex vivo* or *in situ*, reprograms them to mature antigen-presenting cells (18, 19). These DCs and the T cells they activate are protected from regulatory T cells (Treg; ref. 20). These observations, together with the fact that mRNA as a biopharmaceutical fulfills all requirements of an optimal adjuvant, prompted us to evaluate whether i.t. delivery of TriMix mRNA is a feasible strategy to activate TiDCs and as such induce antitumor immunity.

Materials and Methods

Mice

Female 6- to 12-week-old C57BL/6, DBA/2, BALB/c, and OT-1 mice were purchased from Charles River. B. Lambrecht (Ghent University, Belgium) provided CD11c-diphtheria toxin receptor (DTR) mice. V. Flamand (Université Libre de Bruxelles, Belgium)

[1]Laboratory of Molecular and Cellular Therapy (LMCT), Vrije Universiteit Brussel (VUB), Jette, Belgium. [2]In Vivo Cellular and Molecular Imaging Laboratory, VUB, Jette, Belgium. [3]Institut d'Immunologie Médicale, Université Libre de Bruxelles, Gosselies, Belgium.

Note: Supplementary data for this article are available at Cancer Immunology Research Online (http://cancerimmunolres.aacrjournals.org/).

S. Van Lint and D. Renmans contributed equally to this article.

K. Thielemans and K. Breckpot shared senior authorship.

Corresponding Authors: Karine Breckpot, Vrije Universiteit Brussel, Laarbeeklaan 103/E, B-1090, Jette, Brussel 1090, Belgium. Phone: 0032 2 477 45 65; Fax: 0032 2 477 45 68; E-mail: kbreckpo@vub.ac.be; and K. Thielemans, kris.thielemans@vub.ac.be

doi: 10.1158/2326-6066.CIR-15-0163

provided Batf-3$^{-/-}$ mice. Animals were treated according to the European guidelines. The institute's ethical committee for use of laboratory animals approved the experiments.

Mouse cell lines, DCs, and peptides

The E.G7-OVA T-cell lymphoma, the A20 B-cell lymphoma, and the P815 mastocytoma cell lines were obtained from the ATCC in 2013. The lung epithelial cell line TC-1 was provided by T.C. Wu (John Hopkins Medical Institution, Baltimore, MD) in 2012 and authenticated by RT-PCR for the expression of the HPV E7 antigen. Mouse DCs were generated as described (21). Cell lines were thawed within 1 week after arrival, and 10 aliquots of 5×10^6 cells were frozen as soon as feasible. Cells were passaged for less than 3 weeks after thawing. The peptides SIINFEKL (ovalbumin, OVA) and SVYDFFVWL (Trp2) were purchased from Eurogentec (Belgium), whereas P. Coulie (Université Catholique de Louvain, Belgium) provided LPYLGWLVF (P1A) and GYCGLRGTGV (P1E).

mRNA

The vectors pAT1-FLuc (Firefly luciferase), pGEM-tNGFR (truncated nerve growth factor receptor), pST1-eGFP (enhanced green fluorescent protein), pST1-mouse-CD40L-OPT, pST1-mouse-CD70-OPT, and pST1-caTLR4-OPT have been described (19). A codon-optimized version of the *Mus musculus* Thy1.1 gene was purchased from GeneArt (Life Technologies) and cloned as an NcoI-XhoI fragment in the vector pEtheRNA-v2. Prior to *in vitro* transcription, plasmids pAT1, pGEM, pST1, and pEtheRNA-v2 were linearized with AclI, SpeI, SapI, and BfuAI, respectively (Fermentas). *In vitro* mRNA transcription and quality control were performed as described (22).

Tumor cell inoculation and i.t. delivery of mRNA

Mice were injected subcutaneously (50 μL) with 2×10^4 TC-1 cells or 5×10^5 E.G7-OVA, P815, or A20 cells at the lower back or both flanks. Tumors that reached a volume of ± 100 mm^3 as measured by caliper and determined by the formula for a prolate ellipsoid were injected with mRNA resuspended in 50 μL 0.8 Hartmann solution (23).

***In vivo* bioluminescence imaging**

To assess i.t. delivery of mRNA and the cells involved in its uptake, tumors grown in wild-type, Batf-3$^{-/-}$, or CD11c-DTR mice were injected with 10 μg FLuc mRNA. CD11c-DTR mice were treated a day before mRNA delivery with PBS or 4 ng DT/gram bodyweight (Sigma-Aldrich). *In vivo* bioluminescence imaging (BLI) was performed at the indicated time points (24).

Tracking of *in vivo* mRNA-transfected cells

Twenty-four hours before their isolation, tumors were injected with 10 μg Thy1.1 mRNA. Single cells were stained with antibodies specific for Thy1.1 coupled to phycoerythrin (PE; clone OX7; Becton Dickinson, BD), CD11c-AlexaFluor647 (clone N418; Biolegend), CD11b-FITC (clone M1/70; BD), CD90.2-FITC (clone 30H-12; BD), and F4/80-biotin (prepared in-house and detected with streptavidin-FITC; BD). Staining was performed in the presence of antibodies to CD16/CD32 (BD). Data were collected on the BD LSR Fortessa flow cytometer and analyzed using FACSDiva software (BD). Samples stained with isotype-matched antibodies were used to delineate Thy1.1$^+$ cells.

***In vivo* proliferation assay**

A day before treatment, 1×10^6 MACS-sorted (Miltenyi Biotec) and 0.5 μmol/L carboxyfluorescein diacetate succinimidyl ester (CFSE)–labeled (Life Technologies) CD8$^+$ OT-1 T cells were injected intravenously (200 μL PBS). Tumors were treated with 40 μg tNGFR mRNA, 10 μg tNGFR and 30 μg TriMix mRNA (10 μg/component), 10 μg OVA and 30 μg TriMix mRNA, or 10 μg OVA and 30 μg tNGFR mRNA. The presence and phenotype of CFSE^{low} T cells in tumor-draining lymph nodes (TDLN) and tumors were analyzed 5 days later by flow cytometry. Cells were stained with peridinin-chlorophyll proteins (PerCP-Cy5.5)–conjugated antibodies to CD8 (clone 53–6.7; BD) together with antibodies to CD62L-PE-Cy7 (clone MEL-14; BD) and CD44-AF647 (clone IM7; BioLegend), antibodies to CD25-PE (clone 3C7; BD) and CD69-allophycocyanin (APC; clone H1.2F3; BD), or antibodies to CD27-APC (clone LG.7F9; eBioscience) and PD-1-PE (clone RMPI-30; BioLegend). Perforin was stained intracellularly using antibodies to perforin–PE (clone eBIOMAK-D; eBioscience). Isotype-matched antibodies (BD) were used to verify staining specificity and to delineate positive populations. Data were collected using the BD LSR Fortessa flow cytometer. Analyses were performed with the FACSDiva software (BD). A light scatter gate excluding death lymphocytes and additional gating on CD8$^+$CFSE^{low} cells was used.

IFNγ ELISPOT assay

Tumors were injected with 30 μg tNGFR or TriMix mRNA (10 μg/component). Five days later, CD8$^+$ T cells were MACS-sorted from TDLNs. CD8$^+$ T cells (2×10^5) were stimulated in duplicate for 3 days with 5 μmol/L of the appropriate peptide in a 96-well multiscreen PVDF-membrane plate (Millipore). Control peptides and CD8$^+$ T cells obtained from LNs of naïve mice were used for comparison. As a positive control, CD8$^+$ T cells were stimulated with mouse CD3/CD28 antibody–coated beads (1/100; Invitrogen). The ELISPOT was performed following the manufacturer's instructions (Cell Sciences).

***In vivo* cytotoxicity assay**

Tumors were injected with 30 μg tNGFR or TriMix mRNA (10 μg/component), or 20 μg tNGFR and 10 μg caTLR4 mRNA. When indicated, tumors were further injected with 10 μg tNGFR or OVA mRNA. CD11c-DTR mice were treated intraperitoneally with PBS or 4 ng DT/g body weight a day before treatment. When indicated, mice received 25 μg FTY-720 (Enzo Life Sciences) by oral gavage (200 μL) 4 hours before treatment. The *in vivo* cytotoxicity assay was performed as described (19).

Therapy experiments

Tumors were injected with 30 μg tNGFR or TriMix mRNA (10 μg/mRNA), or 20 μg tNGFR and 10 μg caTLR4 mRNA. When indicated, mice received 25 μg FTY-720 as described above. Tumor length and width were measured using a caliper, and volumes were calculated using the formula for a prolate ellipsoid. Mice were killed when tumors exceeded 1,500 mm^3.

***In vivo* migration of DCs**

Bone marrow–derived DCs were electroporated with 10 μg FLuc or eGFP mRNA (25). Four hours before injecting 30 μg tNGFR or TriMix mRNA, 2×10^6 DCs (50 μL) were administered to tumors. Migration of FLuc$^+$ or eGFP$^+$ DCs to TDLNs

was evaluated 24 hours later using *ex vivo* BLI on TDLNs or flow cytometry analysis on cell suspensions of TDLNs, respectively (26). Staining was performed after blocking Fc receptors with CD16/CD32 antibodies, using anti–CD11c-AF647, biotinylated anti-CD40 (clone FGK45), and anti-CD86 (clone GL-1). Biotinylated antibodies were prepared in-house and detected with SA-PerCP-Cy5.5 (BioLegend) or SA-eFluor450 (eBioScience). Isotype-matched antibodies served as controls (BD). Data were collected and analyzed as described in Supplementary Fig. S1.

In vitro proliferation assay

Tumors were injected with 30 μg tNGFR or TriMix mRNA (10 μg/component). Three days later, $CD11c^+$ cells were MACS-enriched from TDLNs. These were cocultured in duplicate at a 1:10 ratio with 2×10^5 MACS-sorted and 0.5 μmol/L CellTrace Violet–labeled $CD8^+$ OT-1 cells (Life Technologies). Cell proliferation was analyzed 3 days later by flow cytometry. Supernatants were screened in a sandwich ELISA for the presence of IFNγ (eBioscience).

Statistical analyses

A nonparametric Mann–Whitney *U* test or one-way ANOVA followed by Bonferroni correction was performed to compare two or multiple datasets, respectively. Sample sizes are indicated in the figure legends and represent the summary of at least two independent experiments. Numbers of asterisks in the figures indicate the level of statistical significance: *, $P < 0.05$; **, $P < 0.01$; ***, $P < 0.001$. Results are shown in a column graph as mean ± SEM. Survival was visualized in a Kaplan–Meier plot. Differences in survival were analyzed by the log-rank (Mantel Cox) test.

Results

$CD8\alpha^+$ TiDCs engulf mRNA

To address whether cells in the tumor microenvironment engulf mRNA, we injected tumors of different histologic origin in genetically distinct immunocompetent hosts with FLuc mRNA. *In vivo* BLI was performed 24 hours later, showing FLuc expression in E.G7-OVA, P815, TC-1, and A20 tumors (Fig. 1A). Fluorescence

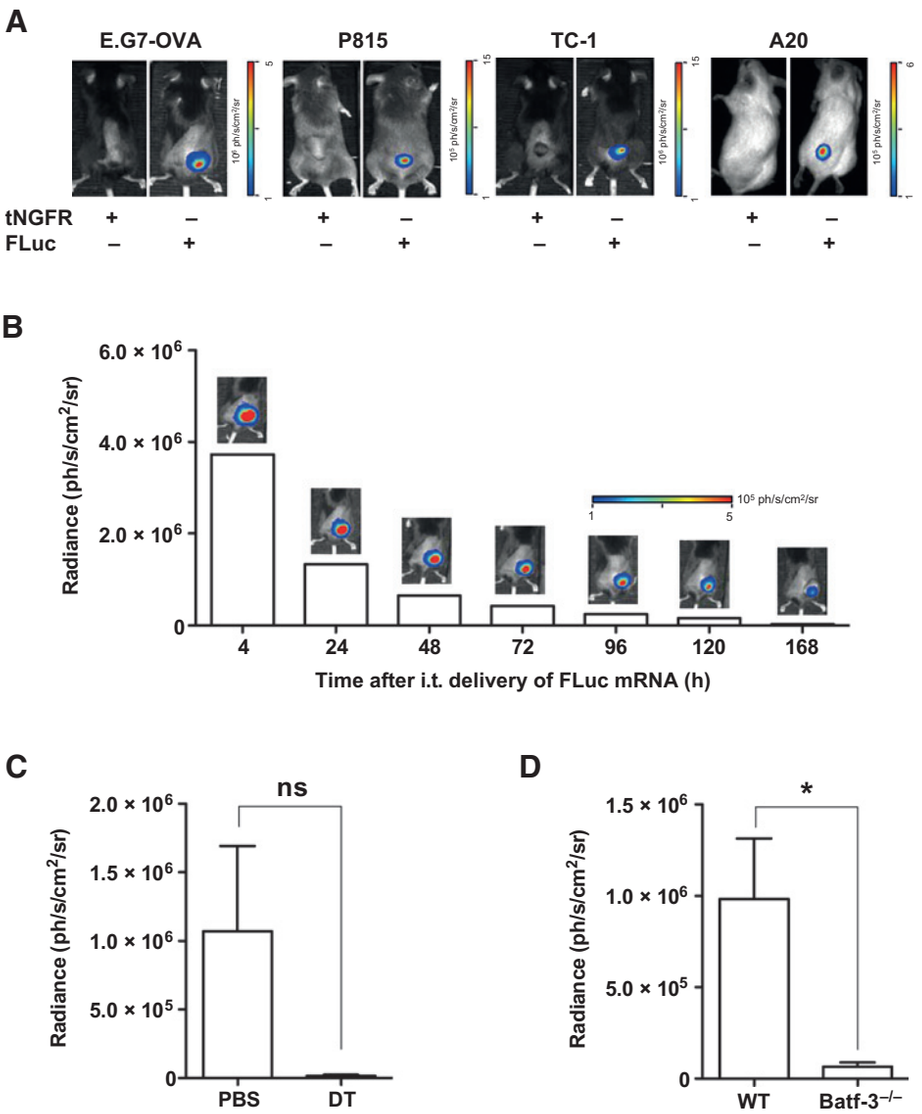

Figure 1.
$CD8\alpha^+$ TiDCs engulf mRNA. A, E.G7-OVA, P815, A20, and TC-1 tumors were injected with 10 μg tNGFR or FLuc mRNA when they reached a volume of ±100 mm^3. *In vivo* BLI was performed 24 hours later ($n = 4$). B, *in vivo* BLI was performed at the indicated time points after injection of 10 μg FLuc mRNA in E.G7-OVA tumors. One representative experiment of four is shown. C, E.G7-OVA–bearing CD11c-DTR mice were treated with PBS or DT, 24 hours before i.t. delivery of 10 μg FLuc mRNA. *In vivo* BLI was performed 4 hours later ($n = 8$). D, E.G7-OVA–bearing wild-type (WT) or Batf-$3^{-/-}$ mice were injected i.t. with 10 μg FLuc mRNA. *In vivo* BLI was performed 24 hours later ($n = 8$). The graphs in C and D summarize the results as mean ± SEM of the indicated number of mice. *, $P < 0.05$; ns, not statistically significant.

at the tumor site was readily detectable in the E.G7-OVA model for about 10 hours (Fig. 1B). Flow cytometry was performed on cell suspensions of P815 tumors injected with Thy1.1 mRNA, showing that a small percentage of mainly $CD11c^+$ cells were $Thy1.1^+$ (data not shown). Mice bearing E.G7-OVA–CD11c-DTR tumors were treated with DT to deplete $CD11c^+$ cells. Uptake of mRNA, as assessed by BLI, was inhibited, which confirmed the role of $CD11c^+$ cells (Fig. 1C). *In vivo* BLI performed on E.G7-OVA–bearing Batf-$3^{-/-}$ mice, which lack $CD8\alpha^+$ DCs, showed significantly reduced radiance compared with wild-type mice, showing that these cross-presenting DCs are mainly responsible for mRNA uptake (Fig. 1D).

TriMix stimulates functional tumor-specific T cells

As cross-presenting $CD8\alpha^+$ TiDCs are at least partially responsible for mRNA uptake, we evaluated whether i.t. delivery of TriMix mRNA results in stimulation of tumor-specific T cells (Fig. 2). We first assessed proliferation by transferring CFSE-labeled $CD8^+$ OT-1 cells into E.G7-OVA–bearing mice and studying their expansion. The OT-1 T cells in the TDLNs of mice treated with TriMix mRNA expanded significantly more than OT-1 cells in mice treated with tNGFR mRNA. Immunization with antigen mRNA alone did not result in a significant change in proliferation compared with immunization with the tNGFR mRNA, hinting that TiDCs have access to TAAs but are dysfunctional. Moreover, coadministration of OVA and TriMix mRNA did not boost OT-1 expansion compared with TriMix delivery alone (Fig. 2A). Nonetheless, antigen presentation is critical, as i.t. injection of TriMix mRNA in mice bearing EL4 tumors (OVA^-) did not induce significant proliferation of OT-1 cells (Supplementary Fig. S2A).

Second, we analyzed the phenotype of proliferating OT-1 cells in E.G7-OVA–bearing mice treated with tNGFR or TriMix mRNA. These were $CD25^+CD44^{high}CD69^+CD62L^{low}$ in both TDLNs and tumors irrespective of the treatment. However, $CFSE^{low}$ OT-1 cells in tumors were $CD27^-PD\text{-}1^+$, which is in contrast with those in TDLNs. $CFSE^{low}$ OT-1 cells in TriMix-treated mice showed a higher expression of perforin compared with those in mice treated with tNGFR mRNA (81.2% ± 1.2% and 44.8% ± 2.8%,

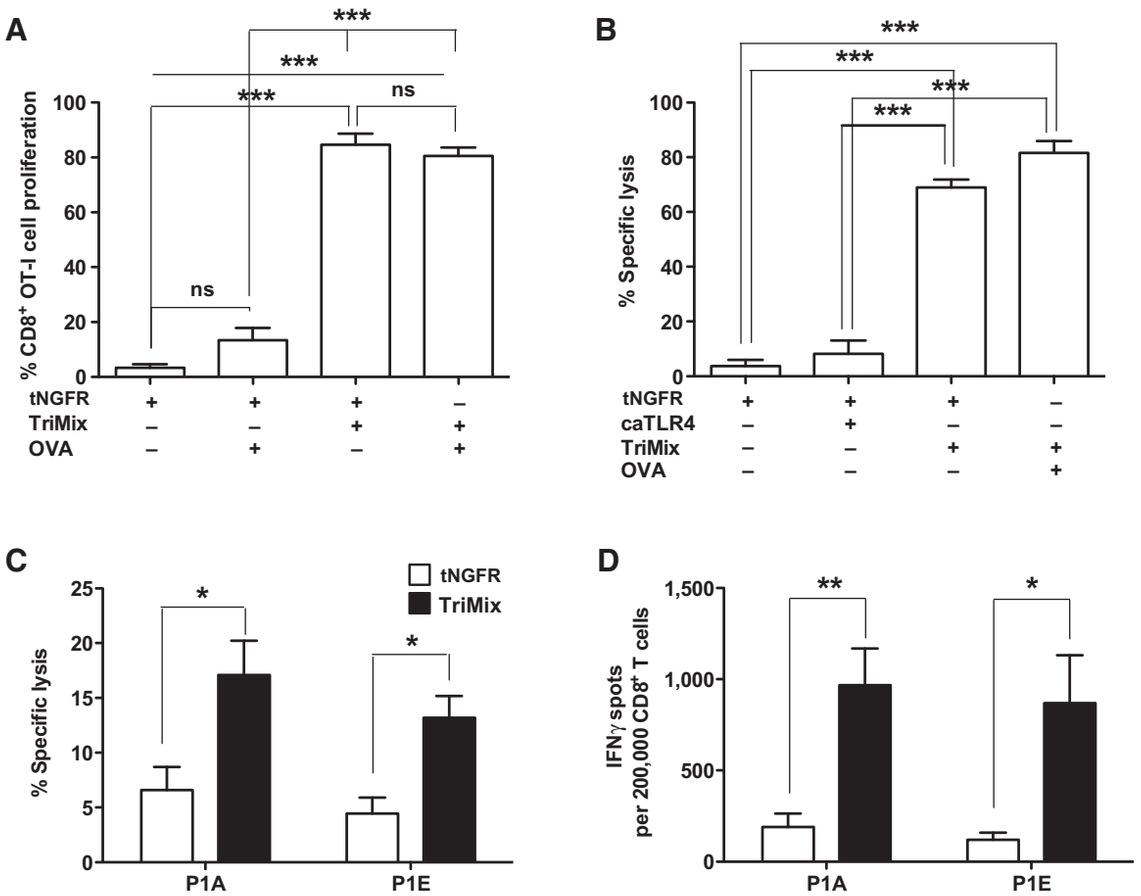

Figure 2.

Intratumoral delivery of TriMix mRNA results in expansion of functional tumor-specific T cells. A, an *in vivo* OT-1 proliferation assay was performed in E.G7-OVA–bearing mice treated with an i.t. injection of 40 μg tNGFR mRNA, 30 μg TriMix mRNA supplemented with 10 μg tNGFR or OVA mRNA, or 30 μg tNGFR mRNA supplemented with 10 μg OVA mRNA. Proliferation of CFSE-labeled OT-1 cells was analyzed in flow cytometry ($n = 5$). B, stimulation of OVA-specific CTLs was analyzed in E.G7-OVA–bearing mice treated with 40 μg tNGFR mRNA, 30 μg tNGFR and 10 μg caTLR4 mRNA, 30 μg TriMix mRNA with 10 μg of tNGFR or OVA mRNA ($n = 10$). The graph in B shows the specific lysis and summarizes the data ($n = 6$). C, stimulation of P1A and P1E-specific CTLs was analyzed in P815-bearing mice treated with 30 μg tNGFR or TriMix mRNA. C, specific lysis and summary of the data ($n = 12$). D, 5 days after i.t. delivery of 30 μg tNGFR or TriMix mRNA in P815-bearing mice, an IFNγ ELISPOT assay was performed. The graph shows the IFNγ spots per 200,000 T cells and summarizes the data ($n = 6$). All graphs show data as mean ± SEM. *, $P < 0.05$; **, $P < 0.01$; ***, $P < 0.001$; ns, not statistically significant.

respectively, $P < 0.001$; Supplementary Fig. S2B and S2C). Therefore, we next evaluated the ability of i.t. TriMix mRNA delivery to induce tumor-specific CTLs and compared it with CTL induction after delivery of caTLR4 or tNGFR mRNA (Fig. 2B). Whereas caTLR4 or tNGFR mRNA injection induced specific lysis of target cells of 8.2% ± 2.0% and 3.7% ± 0.9%, respectively, we found that i.t. injection of TriMix mRNA led to 69.0% ± 1.2% of specific lysis, indicating induction of more CTLs. We also evaluated whether addition of OVA mRNA to TriMix would lead to a higher induction of CTLs, but found this was not the case. We confirmed these results in the P815 model (Fig. 2C), where we found that we could induce CTLs against P1A, a cancer-testis antigen, and P1E, a tumor-specific antigen resulting from a mutation in the methionine sulfoxide reductase gene.

Finally, we evaluated the capacity of the stimulated T cells to produce IFNγ upon restimulation using ELISPOT and found that there was a significantly higher number of IFNγ-producing $CD8^+$ T cells in TriMix mRNA–treated mice, compared with tNGFR mRNA–treated mice in both the P815 (Fig. 2D) and E.G7-OVA (Supplementary Fig. S2D) models.

Intratumoral delivery of TriMix mRNA significantly delays tumor growth

We next assessed the therapeutic potential of i.t. TriMix mRNA delivery. We showed prolonged survival in mice treated with TriMix mRNA compared with mice treated with tNGFR mRNA in various tumor models (Fig. 3A–D). When we evaluated the effect of i.t. injection of caTLR4 mRNA in the P815 model, we observed that these tumors followed the same growth curve as tumors treated with tNGFR mRNA (data not shown). Encouraged by the results obtained with TriMix mRNA, we next used a two-sided tumor model. Herein, only the left tumor was treated while the contralateral tumor (the "control" in Fig. 4) was used to evaluate the induction of systemic antitumor immunity. Treatment with TriMix mRNA resulted in a reduced growth of both A20 and P815 tumors, consequently prolonging survival (Fig. 4A–D).

Antitumor immunity upon i.t. delivery of TriMix mRNA depends on DCs

To study the role of TiDCs in the outcome of i.t. delivery of TriMix mRNA, we used E.G7-OVA–bearing Batf-$3^{-/-}$ mice, which lack splenic $CD8\alpha^+$ DCs. The therapeutic effect of i.t. injection of TriMix mRNA in these mice was dampened (Fig. 5A and B). The lower therapeutic benefit in mice lacking $CD8\alpha^+$ DCs was explained by their lower CTL stimulation, as shown in an *in vivo* cytotoxicity assay (Fig. 5C). Similarly, CTL induction upon i.t. delivery of TriMix mRNA was abrogated when mice lacked $CD11c^+$ cells (Fig. 5D).

Stimulation of T cells upon i.t. delivery of TriMix mRNA occurs in TDLNs

We next addressed whether CTLs are activated in the tumor and/or in the TDLNs. First, we set up a model to evaluate migration of DCs to TDLNs upon i.t. delivery of TriMix mRNA.

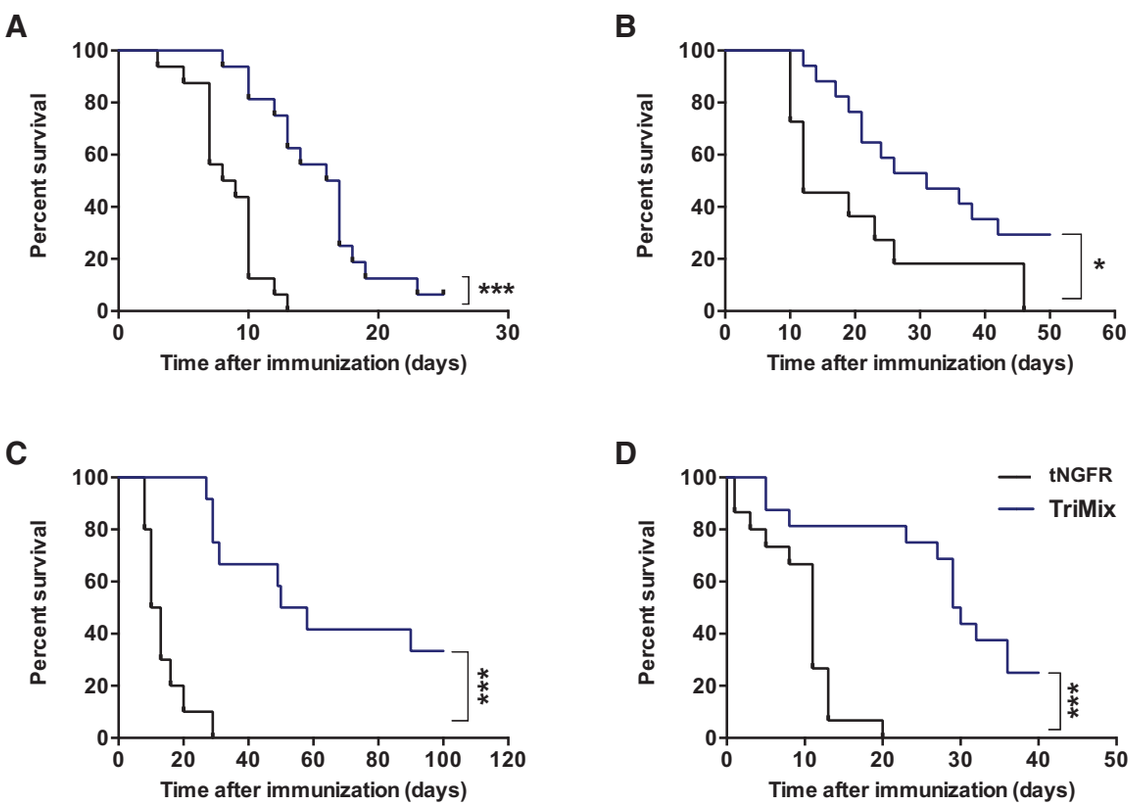

Figure 3.
Delivery of TriMix mRNA to tumors significantly delays their growth. A–D, mice were injected subcutaneously with E.G7-OVA (A), P815 (B), A20 (C), or TC-1 (D) cells. Tumors that reached a size of ± 100 mm^3 were injected with 30 μg tNGFR or TriMix mRNA. Mice were killed when tumors reached a size of ±1,500 mm^3. The survival curves depict pooled results from at least two independent experiments with 5 to 7 mice/group in each experiment. *, $P < 0.05$; ***, $P < 0.001$.

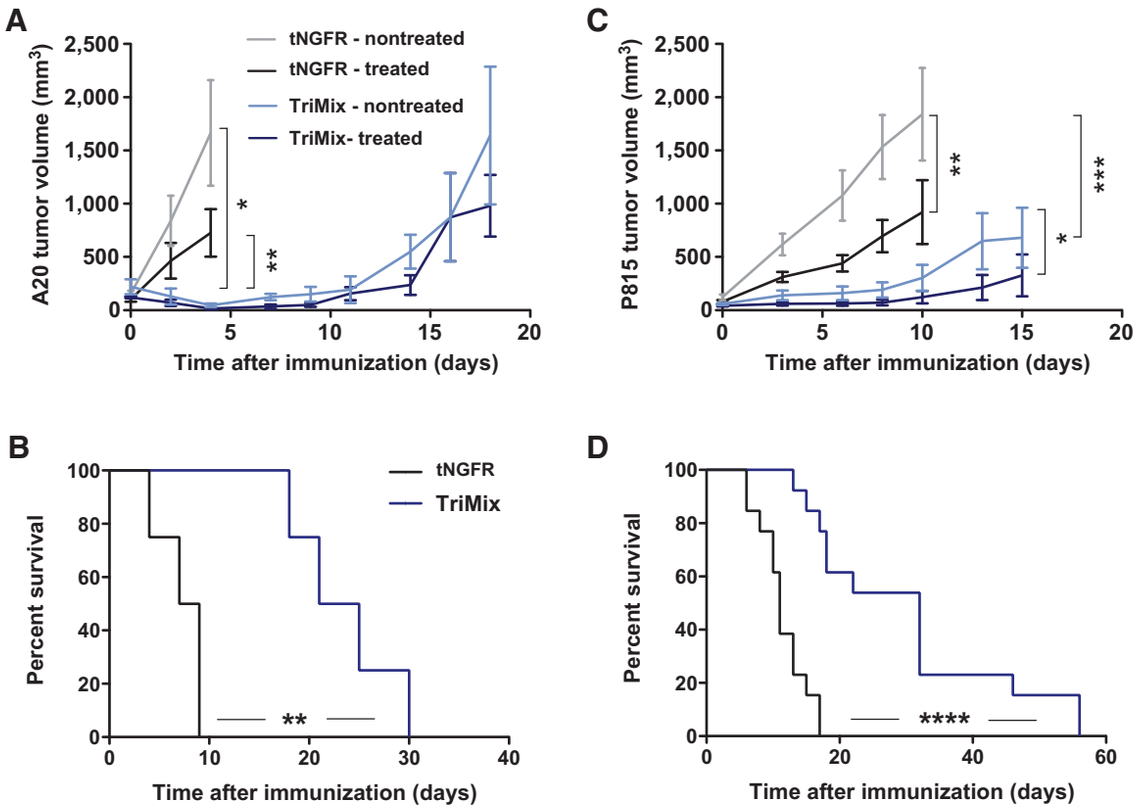

Figure 4.

Intratumoral delivery of TriMix mRNA induces systemic therapeutic responses. A–D, mice were inoculated with tumor cells in both flanks. Once both tumors reached a size of ±100 mm^3, the left tumor was injected with 30 μg tNGFR or TriMix mRNA. A and C, the growth of, respectively, A20 and P815 tumors after treatment with tNGFR or TriMix mRNA is shown for the treated and distant nontreated tumors. B and D, the survival of mice bearing, respectively, A20 or P815 tumors is shown. Results from two experiments with 6 mice/group were pooled for the P815 model. One experiment with 4 mice/group was performed for the A20 model. *, $P < 0.05$; **, $P < 0.01$; ***, $P < 0.001$; ****, $P < 0.0001$.

Tumors were injected with $FLuc^+$ DCs before treatment. Upon i.t. delivery of TriMix mRNA, $FLuc^+$ DCs migrated into the TDLNs in the E.G7-OVA (Fig. 6A) and P815 (data not shown) models, as measured by *ex vivo* BLI. To characterize DCs that entered TDLNs, we used $eGFP^+$ DCs and flow cytometry. The TDLNs of mice treated with TriMix mRNA had a higher percentage of CD40- and CD86-expressing $eGFP^+$ DCs when compared with mice treated with tNGFR mRNA (Fig. 6B and C; Supplementary Fig. S2). This supports the hypothesis that TriMix mRNA induces *in situ* activation and migration of TiDCs. We further stimulated OVA-specific $CD8^+$ T cells *in vitro* with $CD11c^+$ cells sorted from TDLNs of E.G7-OVA–bearing mice treated with tNGFR or TriMix mRNA. We demonstrated enhanced T-cell proliferation (Fig. 6D) and IFNγ secretion (data not shown), indicating that T-cell stimulation could occur in TDLNs.

These data, however, do not exclude the possibility that T cells are activated at the tumor site as well. Therefore, we evaluated the induction of CTLs in E.G7-OVA–bearing mice treated with tNGFR or TriMix mRNA from which the TDLN had been resected 3 days before treatment. CTL induction in these mice was dramatically decreased (Fig. 7A). Nonetheless, mice from which the TDLNs were removed and that were treated with TriMix mRNA showed a prolonged survival (Fig. 7B), suggesting that tumor-infiltrating T lymphocytes (TIL) could be reactivated upon i.t. delivery of TriMix mRNA. To study this, we pretreated tumor-bearing mice with FTY-720, an agonist of the sphingosine 1-phosphate receptor that abrogates the egress of T cells (27). In these mice, treatment of tumors with TriMix mRNA did not stimulate tumor-specific CTLs (Fig. 7C). FTY-720 pretreatment only marginally affected the therapeutic potential of i.t. treatment with TriMix mRNA, supporting the hypothesis that i.t. delivery of TriMix mRNA results in *de novo* activation of tumor-specific T cells as well as reactivation of TILs (Fig. 7D).

Discussion

In most human and mouse solid cancers, the tumor microenvironment is infiltrated with DCs. These TiDCs acquire TAAs; however, they are unable to present them to and properly activate CTLs. This dysfunction is due to immunosuppressive factors present in the tumor microenvironment (28). Several strategies aimed at improving the function of TiDCs have been developed. Examples are the use of TLR agonists and agonistic CD40 antibodies. However, TLRs and CD40 are not exclusively expressed on DCs, and negative signaling resulting in tumor immune escape and tumor cell dissemination has been described (3, 6, 7). Consequently, strategies need to be developed that mediate selective activation of TiDCs. Here, we show that TriMix mRNA reprograms

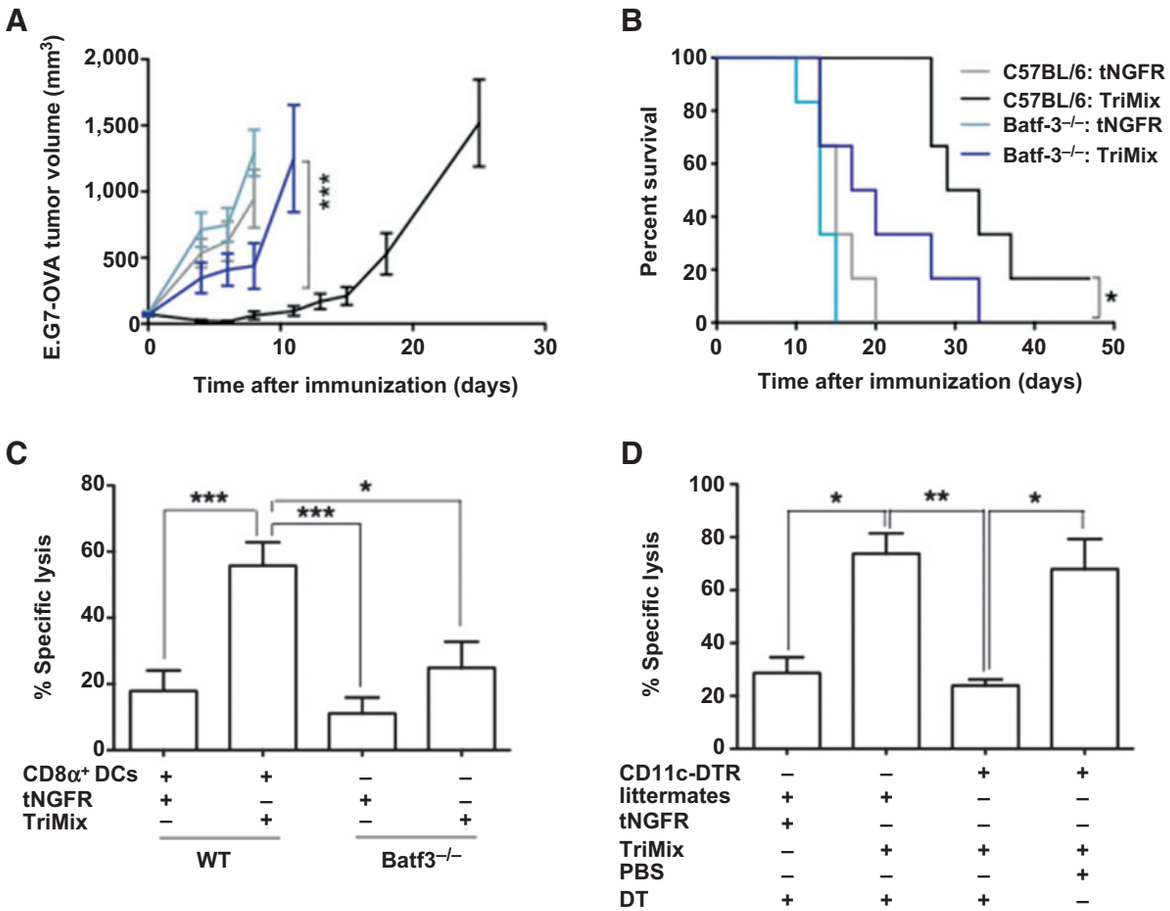

Figure 5.
Induction of antitumor immunity upon i.t. delivery of TriMix mRNA depends on DCs. A and B, tumor growth of E.G7-OVA–bearing Batf-3$^{-/-}$ and WT mice treated with 30 μg tNGFR or TriMix mRNA was followed. A, the mean tumor volume is shown; B, the survival of mice ($n = 6$). C and D, induction of OVA-specific CTLs was evaluated in an *in vivo* cytotoxicity assay in E.G7-OVA–bearing Batf-3$^{-/-}$mice, CD11c-DTR mice, or their littermates treated as in A. The latter two were treated with DT 1 day prior and 2 days after mRNA delivery. The graphs in C and D show the specific lysis as mean ± SEM. *, $P < 0.05$; **, $P < 0.01$; ***, $P < 0.001$.

CD8α$^+$ TiDCs *in vivo* into stimulatory cells that efficiently process spontaneously engulfed TAAs, upregulate costimulatory molecules, and migrate to TDLNs to activate CTLs. Moreover, we provide evidence that i.t. delivery of TriMix mRNA results in reactivation of TILs. Together, this results in a delay in growth of established tumors.

We showed that upon i.t. delivery of mRNA, the encoded antigen is mostly but not exclusively expressed in Batf-3–dependent CD11c$^+$ cells. This finding is consistent with several studies showing that Batf-3$^{-/-}$ mice, which lack CD8α$^+$ cross-presenting DCs, fail to clear highly immunogenic tumors (8, 9). Our study confirms that CD8α$^+$ TiDCs have spontaneously acquired TAAs but fail to induce antitumor immunity, unless activated with TriMix mRNA. We furthermore show that induction of CTLs and control of tumor growth are exerted by Batf-3–dependent CD8α$^+$ DCs as well as CD11c$^+$ Batf-3–independent cells. Based on the current knowledge on DC subsets (15), we contend that CD11b$^+$ CD11c$^+$ DCs could play a role, despite their weak *in vitro*–stimulatory properties (29).

Our work further suggests that i.t. delivery of TriMix mRNA results in *de novo* activation of tumor-specific CTLs and reactivation of TILs. Broz and colleagues (29) also showed that Batf-3–dependent cells play a key role in reactivating TILs. Whereas that study shifts the emphasis for T-cell control from TDLNs to tumors, our data show that both the tumor and TDLNs are critical for CTL induction (30–32). However, we cannot exclude that *de novo* T cells trigger a cascade of events at the tumor, resulting in revival of TILs, as previously proposed (33). Therefore, we suggest that i.t. delivery of TriMix mRNA activates tumor-specific T cells *de novo* and results in reactivation of TILs, probably because of their contact with TriMix-modified TiDCs as well as a cascade of TIL-reviving events instigated by *de novo* tumor-specific T cells.

A key point is that the activation of CTLs upon i.t. delivery of TriMix mRNA depends on the spontaneous acquisition of TAAs by TiDCs, avoiding the need to prime TiDCs with exogenous TAAs. Intratumoral delivery of TriMix eliminates the challenge of trying to define the best-suited TAA for vaccination. In this regard, cancer-testis and differentiation antigens are often used. These are self-proteins and are thus subjected to tolerance mechanisms. In contrast, mutated antigens are not in the cross-line of tolerance mechanisms (34–36). Therefore, the use

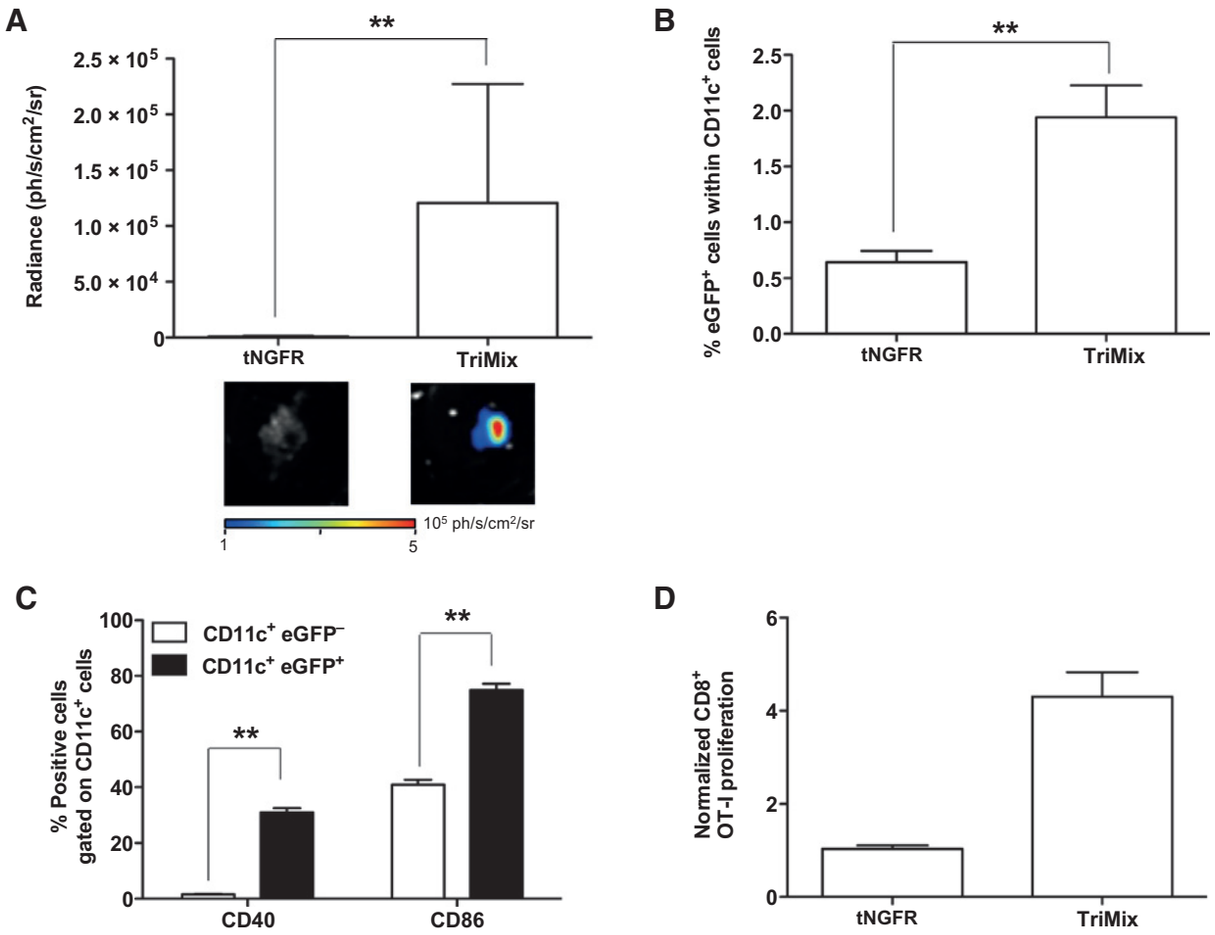

Figure 6.

Intratumoral delivery of TriMix mRNA reprograms TiDCs. A, E.G7-OVA tumors were injected with 2×10^6 FLuc$^+$ DCs 4 hours before their treatment with 30 μg tNGFR or TriMix mRNA. TDLNs were analyzed 24 hours later using *ex vivo* BLI. The graph summarizes the results as mean ± SEM, whereas the photos are representative luminescence images ($n = 6$). B and C, E.G7-OVA tumors were injected with 2×10^6 eGFP$^+$ DCs 4 hours before treatment. TDLNs were analyzed 24 hours later using flow cytometry. The graphs summarize the results as mean ± SEM ($n = 6$). D, CD11c$^+$ cells were isolated from TDLNs 3 days after injection of E.G7-OVA tumors with 30 μg tNGFR or TriMix mRNA and used to stimulate OVA-specific CFSE-labeled CD8$^+$ OT-1 cells. The graph shows proliferation of OT-1 cells in TriMix mRNA–treated mice normalized to that in tNGFR mRNA–treated mice as mean ± SEM ($n = 10$). *, $P < 0.05$.

of the tumor's antigenic repertoire, including neoepitopes, is an attractive approach. We provide evidence that i.t. delivery of TriMix mRNA induces CTLs specific for cancer-testis antigens as well as for a neoepitope. TriMix-activated TiDCs thus have the potential to present a variety of antigens that they acquire at the tumor site.

Large numbers of tumor-specific T cells expanded in mice treated with TriMix mRNA, relative to the expansion in mice treated with tNGFR mRNA. The T cells had a comparable phenotype, characterized by high expression of CD25, CD44, and CD69, and low expression of CD62L and CD27. It is suggested that CD27$^-$ T cells represent a memory subset with cytolytic capacity (37). In this regard, we observed that perforin expression was significantly higher in mice treated with TriMix mRNA. Therefore, it is not surprising that tumor-bearing mice treated with TriMix mRNA were able to delay tumor growth, whereas mice treated with tNGFR mRNA were not. This could be attributed to the lower expansion of perforin-positive tumor-specific T cells. Alternatively, one could argue that CTLs stimulated after i.t. delivery of TriMix mRNA are (partially) protected from suppressive mechanisms exerted in the tumor microenvironment. This hypothesis is supported by a previous study showing that CD8$^+$ T cells activated by TriMix mRNA–modified DCs were protected from Tregs (20). Although we did not study T-cell trafficking in detail, our data on the outgrowth of tumors in the two-sided tumor model further suggest that tumor-specific CTLs efficiently screen the body for tumors, irrespective of whether the primary tumor was cured.

The promise of many cancer immunotherapies is often hampered by the difficulties regarding its targeted *in situ* delivery. In our approach, however, CD8α$^+$ TiDCs are the target, and these cells were shown to engulf and translate mRNA dissolved in Hartmann solution. Most likely, the mRNA uptake is mediated by macropinocytosis as described for the mRNA uptake by intranodal DCs (38). Consequently, when targeting DCs *in situ*, mRNA is an attractive vector as it enables selective delivery without prior manipulation. The mRNA itself can trigger several pattern recognition receptors (PRR; ref. 39), whose activation

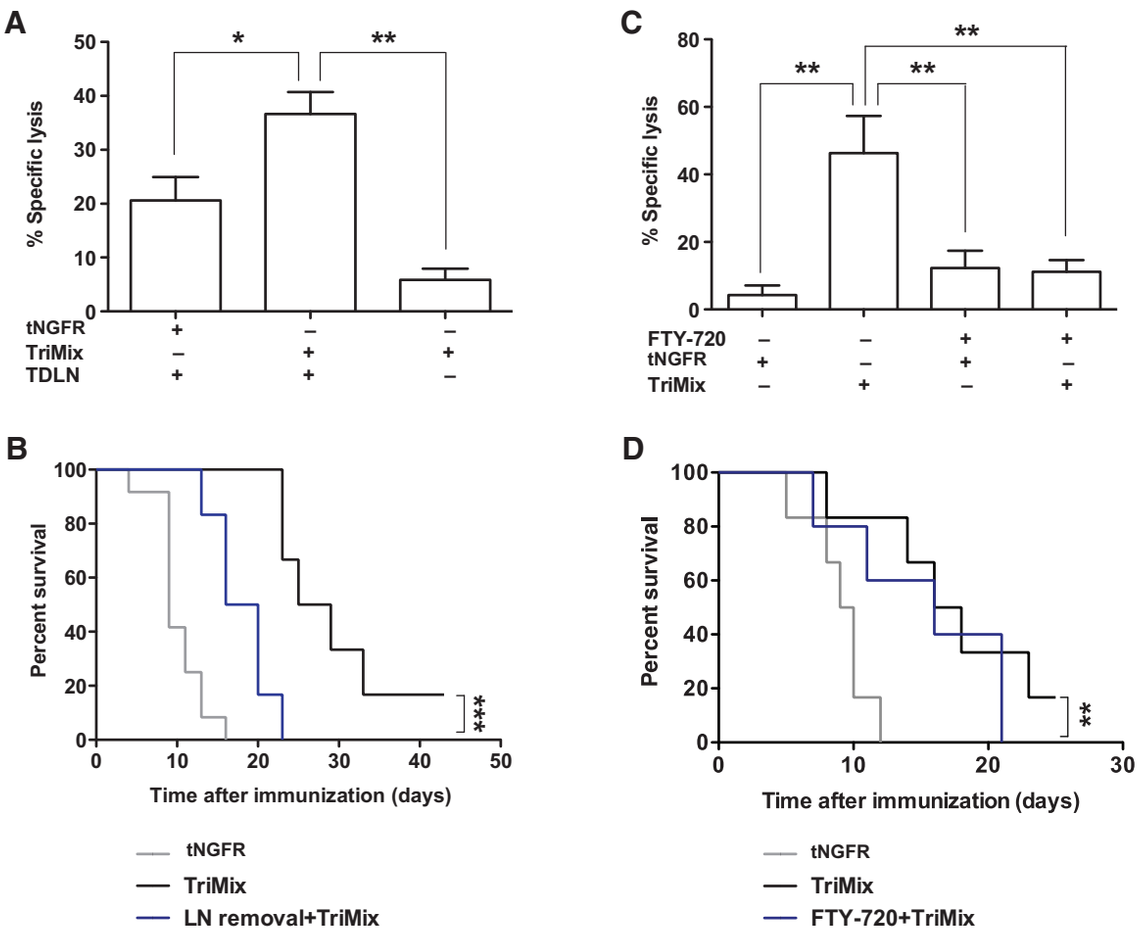

Figure 7.
T-cell stimulation upon i.t. delivery of TriMix mRNA occurs in TDLNs. A, 24 hours before i.t. treatment with 30 μg tNGFR of TriMix mRNA, TDLNs of E.G7-OVA–bearing mice were removed. An *in vivo* cytotoxicity assay was performed. The graph shows the specific lysis as mean ± SEM ($n = 12$). B, mice were treated as described in A, after which tumor growth was monitored. The graph shows the survival of mice ($n = 6$). C, 4 hours before i.t. treatment with 30 μg tNGFR of TriMix mRNA, E.G7-OVA–bearing mice were treated with FTY-720 via oral gavage. An *in vivo* cytotoxicity assay was performed. The graph shows the specific lysis as mean ± SEM ($n = 6$). D, mice were treated as described in C, after which tumor growth was monitored. The graph shows the survival of mice ($n = 6$). *, $P < 0.05$; **, $P < 0.01$; ***, $P < 0.001$.

negatively affects its translation, implying that stronger TiDC activation could be obtained using "modified" mRNA that does not trigger PRRs (40–42). If PRRs are triggered, the effects observed in this study may be due to the delivery of mRNA rather than the delivery of TriMix mRNA. However, when using equal amounts of tNGFR or caTLR4 mRNA, no strong induction of CTLs or therapeutic benefit was seen. These data highlight the added benefit of TriMix mRNA, even if mRNA were to trigger PRRs.

In conclusion, we provide proof-of-concept for the use of TriMix mRNA in i.t. delivery and as such propose a novel cancer immunotherapy that exploits cross-presenting DCs and the tumor's antigenic repertoire to stimulate effective antitumor immune responses.

Disclosure of Potential Conflicts of Interest

C. Heirman is an employee at eTheRNA. K. Thielemans is the holder of a patent for dendritic cells electroporated with tumor antigen mRNA and TriMix (WO2009/034172). No other potential conflicts of interest were disclosed by the other authors.

Authors' Contributions

Conception and design: S. Van Lint, D. Renmans, C. Heirman, K. Thielemans, K. Breckpot

Development of methodology: S. Van Lint, D. Renmans, C. Heirman, K. Thielemans, K. Breckpot

Acquisition of data (provided animals, acquired and managed patients, provided facilities, etc.): S. Van Lint, D. Renmans, K. Broos, L. Goethals, S. Maenhout, S. Du Four, K. Van der Jeught, L. Bialkowski, V. Flamand, K. Breckpot

Analysis and interpretation of data (e.g., statistical analysis, biostatistics, computational analysis): S. Van Lint, D. Renmans, L. Goethals, S. Du Four, K. Van der Jeught, L. Bialkowski, C. Heirman, K. Thielemans, K. Breckpot

Writing, review, and/or revision of the manuscript: S. Van Lint, D. Renmans, K. Broos, L. Goethals, S. Maenhout, C. Goyvaerts, S. Du Four, K. Van der Jeught, L. Bialkowski, V. Flamand, C. Heirman, K. Thielemans, K. Breckpot

Administrative, technical, or material support (i.e., reporting or organizing data, constructing databases): S. Van Lint, S. Du Four, L. Bialkowski, K. Thielemans, K. Breckpot

Study supervision: S. Van Lint, K. Thielemans, K. Breckpot

Acknowledgments

The authors thank Petra Roman and Elsy Vaeremans for their excellent technical assistance.

Grant Support

This study was supported by the grants from the Interuniversity Attraction Poles Program-Belgian State-Belgian Science Policy, the National Cancer Plan of the Federal Ministry of Health, the Belgian Federation against Cancer, the Vlaamse Liga tegen Kanker, the IWT, the FWO-V, an EU FP7-funded Network of Excellence, and the Scientific Fund Willy Gepts (University Hospital Brussels). D. Renmans, K. Broos, S. Maenhout, S. Du Four, L. Bialkowski, and K. Van der Jeught are funded by the IWT; L. Goethals is funded by the Stichting tegen Kanker; and C. Goyvaerts is funded by the FWO-V.

The costs of publication of this article were defrayed in part by the payment of page charges. This article must therefore be hereby marked *advertisement* in accordance with 18 U.S.C. Section 1734 solely to indicate this fact.

Received July 12, 2015; revised October 5, 2015; accepted October 23, 2015; published OnlineFirst December 11, 2015.

References

1. Pinzon-Charry A, Maxwell T, Lopez JA. Dendritic cell dysfunction in cancer: a mechanism for immunosuppression. Immunol Cell Biol 2005;83:451–61.
2. Tran Janco JM, Lamichhane P, Karyampudi L, Knutson KL. Tumor-infiltrating dendritic cells in cancer pathogenesis. J Immunol 2015;194: 2985–91.
3. Van der Jeught K, Bialkowski L, Daszkiewicz L, Broos K, Goyvaerts C, Renmans D, et al. Targeting the tumor microenvironment to enhance antitumor immune responses. Oncotarget 2015;6:1359–81.
4. Singh M, Overwijk WW. Intratumoral immunotherapy for melanoma. Cancer Immunol Immunother 2015;64:911–21.
5. Marabelle A, Kohrt H, Caux C, Levy R. Intratumoral immunization: a new paradigm for cancer therapy. Clin Cancer Res 2014;20:1747–56.
6. Huang B, Zhao J, Li H, He KL, Chen Y, Chen SH, et al. Toll-like receptors on tumor cells facilitate evasion of immune surveillance. Cancer Res 2005;65:5009–14.
7. Chiodoni C, Lezzi M, Guiducci C, Sangaletti S, Alessandrini I, Ratti C, et al. Triggering CD40 on endothelial cells contributes to tumor growth. J Exp Med 2006;203:2441–50.
8. Furumoto K, Soares L, Engleman EG, Merad M. Induction of potent antitumor immunity by in situ targeting of intratumoral DCs. J Clin Invest 2004;113:774–83.
9. Hildner K, Edelson BT, Purtha WE, Diamond M, Matsushita H, Kohyama M, et al. Batf3 deficiency reveals a critical role for CD8alpha+ dendritic cells in cytotoxic T cell immunity. Science 2008; 322:1097–100.
10. Kreutz M, Tacken PJ, Figdor CG. Targeting dendritic cells–why bother? Blood 2013;121:2836–44.
11. Kreutz M, Giquel B, Hu Q, Abuknesha R, Uematsu S, Akira S, et al. Antibody-antigen-adjuvant conjugates enable co-delivery of antigen and adjuvant to dendritic cells in cis but only have partial targeting specificity. PLoS One 2011;7:e40208.
12. Tacken PJ, Zeelenberg IS, Cruz LJ, van Hout-Kuijer MA, van de Glind G, Fokkink RG, et al. Targeted delivery of TLR ligands to human and mouse dendritic cells strongly enhances adjuvanticity. Blood 2011;118: 6836–44.
13. Tacken PJ, Figdor CG. Targeted antigen delivery and activation of dendritic cells in vivo: steps towards cost effective vaccines. Semin Immunol 2011;23:12–20.
14. Goyvaerts C, Broos K, Escors D, Heirman C, Raes G, De Baetselier P, et al. The transduction pattern of IL-12-encoding lentiviral vectors shapes the immunological outcome. Eur J Immunol 2015; 45:3351–61.
15. Goyvaerts C, Breckpot K. Pros and cons of antigen-presenting cell targeted tumor vaccines. J Immunol Res 2015;2015:785634.
16. Goyvaerts C, De Groeve K, Van Lint S, Heirman C, Van Ginderachter JA, De Baetselier P, et al. Immunogenicity of targeted lentivectors. Oncotarget 2014;5:704–15.
17. Bonehill A, Tuyaerts S, Van Nuffel AM, Heirman C, Bos TJ, Fostier K, et al. Enhancing the T-cell stimulatory capacity of human dendritic cells by co-electroporation with CD40L, CD70 and constitutively active TLR4 encoding mRNA. Mol Ther 2008;16:1170–80.
18. Bonehill A, Van Nuffel AM, Corthals J, Tuyaerts S, Heirman C, François V, et al. Single-step antigen loading and activation of dendritic cells by mRNA electroporation for the purpose of therapeutic vaccination in melanoma patients. Clin Cancer Res 2009;15:3366–75.
19. Van Lint S, Goyvaerts C, Maenhout S, Goethals L, Disy A, Benteyn D, et al. Preclinical evaluation of TriMix and antigen mRNA-based antitumor therapy. Cancer Res 2012;72:1661–71.
20. Pen JJ, De Keersmaecker B, Maenhout SK, Van Nuffel AM, Heirman C, Corthals J, et al. Modulation of regulatory T cell function by monocyte-derived dendritic cells matured through electroporation with mRNA encoding CD40 ligand, constitutively active TLR4, and CD70. J Immunol 2013;191:1976–83.
21. Breckpot K, Dullaers M, Bonehill A, van Meirvenne S, Heirman C, de Greef C, et al. Lentivirally transduced dendritic cells as a tool for cancer immunotherapy. J Gene Med 2003;5:654–67.
22. Bonehill A, Heirman C, Tuyaerts S, Michiels A, Breckpot K, Brasseur F, et al. Messenger RNA-electroporated dendritic cells presenting MAGE-A3 simultaneously in HLA class I and class II molecules. J Immunol 2004;172:6649–57.
23. Van der Jeught K, Tjok Joe P, Bialkowski L, Heirman C, Daszkiewicz L, Liechtenstein T, et al. Intratumoral administration of mRNA encoding a fusokine consisting of IFN-beta and the ectodomain of the TGF-beta receptor II potentiates antitumor immunity. Oncotarget 2014;5: 10100–13.
24. Keyaerts M, Verschueren J, Bos TJ, Tchouate-Gainkam LO, Peleman C, Breckpot K, et al. Dynamic bioluminescence imaging for quantitative tumour burden assessment using IV or IP administration of D: -luciferin: effect on intensity, time kinetics and repeatability of photon emission. Eur J Nucl Med Mol Imaging 2008;35:999–1007.
25. Dullaers M, Breckpot K, Van Meirvenne S, Bonehill A, Tuyaerts S, Michiels A, et al. Side-by-side comparison of lentivirally transduced and mRNA-electroporated dendritic cells: implications for cancer immunotherapy protocols. Mol Ther 2004;10:768–79.
26. Breckpot K, Escors D, Arce F, Lopes L, Karwacz K, Van Lint S, et al. HIV-1 lentiviral vector immunogenicity is mediated by Toll-like receptor 3 (TLR3) and TLR7. J Virol 2010;84:5627–36.
27. Zhi L, Kim P, Thompson BD, Pitsillides C, Bankovich AJ, Yun SH, et al. FTY720 blocks egress of T cells in part by abrogation of their adhesion on the lymph node sinus. J Immunol 2011;187:2244–51.
28. Hargadon KM. Tumor-altered dendritic cell function: implications for anti-tumor immunity. Front Immunol 2013;4:192.
29. Broz ML, Binnewies M, Boldajipour B, Nelson AE, Pollack JL, Erle DJ, et al. Dissecting the tumor myeloid compartment reveals rare activating antigen-presenting cells critical for T cell immunity. Cancer Cell 2014;26:638–52.
30. Marzo AL, Lake RA, Lo D, Sherman L, McWilliam A, Nelson D, et al. Tumor antigens are constitutively presented in the draining lymph nodes. J Immunol 1999;162:5838–45.
31. Bai XF, Gao JX, Liu J, Wen J, Zheng P, Liu Y. On the site and mode of antigen presentation for the initiation of clonal expansion of CD8 T cells specific for a natural tumor antigen. Cancer Res 2001;61:6860–7.
32. Hargadon KM, Brinkman CC, Sheasley-O'neill S L, Nichols LA, Bullock TN, Engelhard VH. Incomplete differentiation of antigen-specific CD8 T cells in tumor-draining lymph nodes. J Immunol 2006; 177:6081–90.
33. Coulie PG, Van den Eynde BJ, van der Bruggen P, Boon T. Tumour antigens recognized by T lymphocytes: at the core of cancer immunotherapy. Nat Rev Cancer 2014;14:135–46.
34. Boisguerin V, Castle JC, Loewer M, Diekmann J, Mueller F, Britten CM, et al. Translation of genomics-guided RNA-based personalised cancer vaccines: towards the bedside. Br J Cancer 2014;111:1469–75.
35. Kreiter S, Castle JC, Tureci O, Sahin U. Targeting the tumor mutanome for personalized vaccination therapy. Oncoimmunology 2012;1:768–9.
36. Castle JC, Kreiter S, Diekmann J, Löwer M, van de Roemer N, de Graaf J, et al. Exploiting the mutanome for tumor vaccination. Cancer Res 2012;72:1081–91.

37. Baars PA, Sierro S, Arens R, Tesselaar K, Hooibrink B, Klenerman P, et al. Properties of murine (CD8+)CD27- T cells. Eur J Immunol 2005;35: 3131–41.
38. Diken M, Kreiter S, Selmi A, Britten CM, Huber C, Türeci Ö, et al. Selective uptake of naked vaccine RNA by dendritic cells is driven by macropinocytosis and abrogated upon DC maturation. Gene Ther 2011;18:702–8.
39. Sahin U, Kariko K, Tureci O. mRNA-based therapeutics–developing a new class of drugs. Nat Rev Drug Discov 2014;13:759–80.
40. Anderson BR, Muramatsu H, Jha BK, Silverman RH, Weissman D, Kariko K. Nucleoside modifications in RNA limit activation of 2′-5′-oligoadenylate synthetase and increase resistance to cleavage by RNase L. Nucleic Acids Res 2011;39:9329–38.
41. Anderson BR, Muramatsu H, Nallagatla SR, Bevilacqua PC, Sansing LH, Weissman D, et al. Incorporation of pseudouridine into mRNA enhances translation by diminishing PKR activation. Nucleic Acids Res 2010;38: 5884–92.
42. Kariko K, Muramatsu H, Welsh FA, Ludwig J, Kato H, Akira S, et al. Incorporation of pseudouridine into mRNA yields superior nonimmunogenic vector with increased translational capacity and biological stability. Mol Ther 2008;16:1833–40.